

Critical dynamics of unstable states

Yannis Drossinos

Department of Chemistry, Harvard University, Cambridge, Massachusetts 02138

David Ronis*

Department of Chemistry, McGill University, 801 Sherbrooke Street West, Montreal, Quebec, Canada H3A 2K6

(Received 3 February 1989; revised manuscript received 9 April 1990)

A one-loop, renormalized, non-Markovian equation of motion for the average order parameter of the time-dependent, scalar, nonconserved Landau-Ginzburg model in the critical region is presented. A new time-dependent length scale, a coherence length of critical-like fluctuations, is defined via a memory-dependent dynamic match condition. Two coupled equations for the new length scale and the average order parameter are numerically solved for instantaneous quenches into the unstable region of the phase diagram. The instantaneous free energy that governs the dynamics is not equal to the adiabatic free energy, and the new length scale increases rapidly in regions of negative instantaneous susceptibility. For quenches at zero external field through the critical temperature the structure factor decomposes into two independent parts at intermediate and late times. The late-time contribution is approximately given by a mean-field, critical structure factor. Both contributions admit scaling forms, albeit with different scaling lengths.

I. INTRODUCTION

The time evolution of systems quenched from an initially disordered state into the unstable region of the phase diagram has received considerable attention in the last few years.¹ Most of the recent work is based on Monte Carlo simulations²⁻⁴ and focuses on the growth of domains of the ordered phase and the scaling properties of the structure factor under critical quenches, i.e., quenches at zero external field through the critical temperature. Concurrently, continuum phenomenological theories¹ have been used to study the dynamics of systems quenched anywhere in the unstable region, thereby investigating the importance of pseudospinodals for the time evolution of the order parameter and eventual decay to the final equilibrium state. This work follows the latter approach and considers fluctuation corrections to mean-field dynamics for systems with nonconserved order parameter that are quenched into the unstable region.

Mean-field dynamics show that metastable states have infinite lifetimes⁵ and that a well-defined spinodal curve is the ultimate limit of metastability. More sophisticated theories, however, distinguish two decay mechanisms. According to classical nucleation theory⁶ metastable states have finite lifetimes and decay via finite-amplitude, localized fluctuations (which are viewed as droplets of the new phase), whereas unstable states decay via small-amplitude, long-wavelength fluctuations,⁷ in a process that for systems with conserved order parameter is called spinodal decomposition.

Cluster-dynamics studies⁸ and computer simulations⁹ have shown, however, that systems with short-range interactions do not have a well-defined spinodal curve and that the distinction between the two decay mechanisms is not as sharp as envisioned by mean-field theory. As a consequence, the free energy that governs the dynamic

evolution of the order parameter is assumed to be ill defined, even though it has a well-defined infinite-time limit (which determines the final equilibrium state). Systems with long-range forces are accurately described by mean-field theories and appear to have well-defined spinodals.¹⁰

Analytical approaches to the dynamics of unstable states usually start from linear⁷ or nonlinear Langevin equations and consider fluctuation corrections either by the renormalization-group transformation¹¹ or by deriving a hierarchy of equations for correlations functions, which are then approximately truncated. Langer *et al.*¹² presented one of the first treatments of spinodal decomposition based on the latter approach, using an *ad hoc* factorization scheme to decouple the hierarchy of equations. Their work was criticized and extended to a nonconserved order parameter system by Billotet and Binder,¹³ who argued that two length scales are necessary for a proper description of the dynamics, the thermal correlation length and the average domain size of the nucleating phase, although their calculation only gave one dominant scale. These results are qualitatively similar to those of Kawasaki *et al.*,¹⁴ who performed a resummation of the perturbation expansion, without assuming a bimodal form for the distribution function. The calculation of Ref. 14 produces a bimodal distribution for quenches at zero external field, but the derivation requires that fluctuations with magnitude larger than the mean-field equilibrium value vanish. More recently, Mazenko *et al.*¹⁵ introduced a renormalization-group analysis that incorporates two length scales, and they developed a comprehensive theory for growth kinetics with primary emphasis, however, on critical quenches.

Many of the earlier works⁷⁻¹⁴ do not include couplings to thermal fluctuations nonperturbatively. A key aspect of these calculations is a bimodal order-parameter distri-

bution which, at least for quenches in the absence of a symmetry-breaking external field, becomes strongly peaked around the possible equilibrium values of the order-parameter. Clearly, the bimodal nature of the order-parameter fluctuations will be unimportant if the *distance* between the two equilibrium states becomes comparable to the magnitude of thermal fluctuations, i.e., as the critical point region is approached. Of course, even in the vicinity of the critical point some observables will develop bimodal distributions, e.g., the distribution of the integrated order parameter for a domain of size L should be bimodal, even near critical point, if $L \gg \xi$, where ξ is the thermal correlation length. In addition, the presence of a symmetry-breaking field, in or out of the critical-point region, will affect the degree to which the fluctuations have bimodal character.

In a previous paper,¹⁶ henceforth referred to as I, we presented a quasistatic, one-loop analysis of the metastable region and considered the scaling form of the equation of state for a scalar ϕ^4 Landau-Ginzburg free energy in the metastable region. The results should describe the behavior of the system in the *metastable* region of the phase diagram for times less than the nucleation time.¹⁷ Here we consider the dynamical version of I in the critical region; we shall not, however, explicitly consider droplet fluctuations, which cause metastable states to decay. Thus our calculation is restricted to quenches into the unstable region near the critical point, and, among other things, we defer the study of decay of metastable states to future work.

In I we proposed a modification of the Rudnick-Nelson¹⁸ equation of state that resulted in an equation of state valid in the whole metastable region. Moreover, the introduction of a second length scale, ρ , the scale parameter, independent of the correlation length, ξ (defined as $\xi = \chi^{1/2}$, where χ is the susceptibility) was found to be necessary. The scale parameter was found to diverge along a new line of ϕ^4 fixed points in the thermodynamic phase diagram, the universal spinodal, that was always in the unstable region of the phase diagram ($\chi < 0$).¹⁹

The scale parameter, characterizes regions of space where the fluctuations are like those found at the critical point and where, as at the critical point, nonlinear interactions cannot be treated via naive perturbation theory. (The renormalization group is assumed to effect the required resummations.) The domains characterized by the scale parameter will be isotropic on the average, and therefore the reader might be tempted to conclude that they are the droplets, or clusters often discussed in the theories of spinodal decomposition or ordering and nucleation. On the other hand, the scale parameter will also characterize the width of the interface of the domains, and this will be large. Thus, unlike the theory far from the critical point, here the domains or droplets will have diffuse interfaces, at least for times that are much longer than those found elsewhere.

The primary motivation for this work was an investigation of the significance of the universal spinodal and the scale parameter for the time evolution, phase separation, and eventual decay of unstable states to the final equilibrium state. We consider a scalar, time-dependent

Landau-Ginzburg model for a system with nonconserved order parameter (model A in critical dynamics²⁰). This model has been used to study the statics and dynamics of order-disorder transitions in binary alloys, e.g., Cu_3Au alloys. In Sec. II we define the model and derive a functional integral representation of the Martin-Siggia-Rose (MSR) functional.²¹ The perturbative treatment of the MSR functional follows closely the analysis of renormalized critical dynamics by Bausch *et al.*²² In particular, a perturbative expression for the equation of motion of the average order parameter is derived by treating critical fluctuations in the field-theoretic renormalization-group approach.²³ Divergent quantities are regularized by dimensional regularization²⁴ and ϵ^{-1} poles, where $\epsilon \equiv 4 - d$ and d is the spatial dimension, are eliminated by minimal subtraction.²⁴ The resulting one-loop renormalized equation of motion is nonlocal in time (i.e., non-Markovian).

Section III, where the perturbative expression is made consistent with the renormalization-group equation and canonical dimensional analysis, contains a discussion of the renormalization-group equation. A dynamic match condition, which generalizes the static match condition presented in I, is proposed, and a set of coupled differential equations for the average order parameter and the scale parameter are derived. The two coupled equations are solved numerically for a series of instantaneous external field and temperature quenches and the results are presented in Sec. IV.

Unlike mean-field treatments, when the quadratic coupling constant in the free energy is sufficiently large, we find that the relaxation of the order parameter is non-monotonic due to coupling to the memory-dependent scale parameter. We explain this effect in terms of instantaneous free-energy surfaces, and present some simple scaling relations in Sec. IV A.

For critical quenches we compute the one-loop structure factor and find three time regimes. The early time behavior is similar to that seen in mean-field treatments; in particular, if the quadratic coupling constant is sufficiently small, then exponential growth is observed. At intermediate and late times the structure factor is written as the sum of two terms, both of which admit scaling forms with different scaling lengths. The characteristic length for the intermediate time component does not grow diffusively, and is simply related to the growth of the scale parameter. At late times the structure factor is well approximated by a mean-field structure factor for a quench from an effective initial temperature to the critical temperature. In particular, diffusive growth is observed and the structure factor decays as q^{-2} as $q \rightarrow \infty$. Finally, Sec. V contains a discussion of our results.

II. DYNAMICAL MODEL A

A. Martin-Siggia-Rose functional

We model the dynamical evolution of the nonconserved order parameter and the ensuing phase separation by a nonlinear Langevin equation:

$$\partial_t \Psi(\mathbf{r}, t) = -\lambda \frac{\delta \beta F}{\delta \Psi(\mathbf{r}, t)} + \theta(\mathbf{r}, t), \quad (2.1a)$$

where $\Psi(\mathbf{r}, t)$ is a space- and time-dependent one-component order parameter, λ is a kinetic Onsager coefficient, and $\theta(\mathbf{r}, t)$ is a white-noise, Gaussian random source, which satisfies

$$\langle \theta(\mathbf{r}, t) \rangle = 0, \tag{2.1b}$$

and

$$\langle \theta(\mathbf{r}, t) \theta(\mathbf{r}', t') \rangle = 2\lambda \delta(\mathbf{r} - \mathbf{r}') \delta(t - t'), \tag{2.1c}$$

where we have chosen units such that $k_B T_c = 1$. The free energy, βF , is chosen to be a coarse-grained Landau-Ginzburg free energy,

$$\beta F = \int d\mathbf{r} \left[\frac{1}{2} |\nabla \Psi|^2 + \frac{1}{2} \tau \Psi^2 + \frac{u}{4!} \Psi^4 \right]. \tag{2.1d}$$

The preceding equations define the time-dependent Landau-Ginzburg model for a nonconserved order parameter, which is dynamical model *A* according to the classification of Hohenberg and Halperin.²⁰

The average over the random source in Eq. (2.1a) can be performed by expressing the solution of the stochastic differential equation in terms of a functional integral. The resulting expression is the Martin-Siggia-Rose generating functional,²¹ and is in a form appropriate for the field-theoretic renormalization-group treatment of critical fluctuations. The derivation of the MSR functional and the subtleties associated with the discretization of the Eq. (2.1a) have been discussed extensively in the literature.²² They will not be reproduced here; instead, following Jensen,²⁵ we obtain

$$\Xi[h, \tilde{h}] \propto \left\langle \int D[\Psi] D[\tilde{\Psi}] \exp \left[i \int d\mathbf{r} dt \left[\tilde{\Psi} \left(\partial_t \Psi + \lambda \frac{\delta \beta F}{\delta \Psi} - \theta \right) + \lambda (h \Psi + \tilde{h} \tilde{\Psi}) \right] \right] \right\rangle_{\theta}, \tag{2.2}$$

where the angular brackets denote the average over the random noise, and an unimportant normalization constant is dropped.

Since the random noise appears linearly in the effective Lagrangian, Eq. (2.2), the Gaussian average is easily performed to obtain

$$\Xi[h, \tilde{h}] \propto \int D[\Psi] D[\tilde{\Psi}] \exp \left[i \int d\mathbf{r} dt \left[\tilde{\Psi} \left(\partial_t \Psi + \lambda (-\nabla^2 + \tau) \Psi + \lambda \frac{u}{3!} \Psi^3 + i \lambda \tilde{\Psi} \right) + \lambda (h \Psi + \tilde{h} \tilde{\Psi}) \right] \right]. \tag{2.3}$$

Note that in Eq. (2.3) \tilde{h} adds linearly to the restoring force $\delta \beta F / \delta \Psi$, thereby becoming the physical external field, whereas h lacks any obvious physical interpretation.

As in static critical phenomena²³ the quantity of interest is the Legendre transform of $-\ln[\Xi(h, \tilde{h})]$, i.e., the generating functional of one-particle irreducible diagrams, defined by

$$\Gamma[\langle \Psi \rangle, \langle \tilde{\Psi} \rangle] \equiv -\ln[\Xi(h, \tilde{h})] + i \lambda \int d\mathbf{r} dt (h \langle \Psi \rangle + \tilde{h} \langle \tilde{\Psi} \rangle). \tag{2.4}$$

Vertex functions, namely correlation functions and response functions, are obtained by functional differentiation,

$$-\Gamma^{(i,j)}(\{\mathbf{r}, t\}_i; \{\mathbf{r}', t'\}_j) \equiv \prod_{m=1}^i \frac{\delta}{\delta \Psi(\mathbf{r}_m, t_m)} \prod_{n=1}^j \frac{\delta}{\delta \tilde{\Psi}(\mathbf{r}_n, t_n)} \Gamma[\langle \Psi \rangle, \langle \tilde{\Psi} \rangle] \Big|_{\langle \Psi \rangle=0, \langle \tilde{\Psi} \rangle=0}; \tag{2.5a}$$

in particular, an equation of motion for the average order parameter is implicitly given by

$$i \frac{\delta \Gamma[\langle \Psi \rangle, \langle \tilde{\Psi} \rangle]}{\delta \langle \tilde{\Psi}(\mathbf{r}, t) \rangle} \Big|_{\langle \tilde{\Psi} \rangle=0} = \lambda \tilde{h}(\mathbf{r}, t). \tag{2.5b}$$

B. Renormalized perturbation expansion

Here we consider quenches into the ordered phase that are spatially uniform on the average, with average order parameter $m(t)$. The motion for $m(t)$ is determined by writing the fluctuating space- and time-dependent order parameter as

$$\Psi_{\mathbf{q}}(t) = (2\pi)^d \delta(\mathbf{q}) m(t) + \delta m_{\mathbf{q}}(t), \tag{2.6}$$

where, in addition, fluctuations were decomposed into their spatial Fourier components. The generating functional, Γ , becomes

$$\Gamma[\langle \Psi \rangle, \langle \tilde{\Psi} \rangle] = -i \int dt (\tilde{\Psi}_0(t) \{ \partial_t m(t) + \lambda m(t) [\tau(t) + \frac{1}{6} u m^2(t) \}]) - i \ln \left[\int D \delta m_{\mathbf{q}}(t) D \tilde{\Psi}_{\mathbf{q}}(t) e^{iL_0 + iL_1} \right], \tag{2.7a}$$

where the zero-loop or tree Lagrangian is

$$iL_0 \equiv i \int \frac{dt d\mathbf{q}}{(2\pi)^d} \tilde{\Psi}_{\mathbf{q}}(t) (\{\partial_t + \lambda[q^2 + \tau(t) + \frac{1}{6}um^2(t)]\} \delta m_{-\mathbf{q}}(t) + i\lambda \tilde{\Psi}_{-\mathbf{q}}(t)), \quad (2.7b)$$

and the interaction terms are

$$iL_1 \equiv \frac{i\lambda u}{2} \int \frac{dt_1 d\mathbf{q}_1 d\mathbf{q}_2}{(2\pi)^{2d}} \tilde{\Psi}_{\mathbf{q}_1}(t_1) m(t) \delta m_{\mathbf{q}_2}(t_1) \delta m_{-\mathbf{q}_1-\mathbf{q}_2}(t_1) \\ + \frac{i\lambda u}{3!} \int \frac{dt_1 d\mathbf{q}_1 d\mathbf{q}_2 d\mathbf{q}_3}{(2\pi)^{3d}} \tilde{\Psi}_{\mathbf{q}_1}(t_1) \delta m_{\mathbf{q}_2}(t_1) \delta m_{\mathbf{q}_3}(t_1) \delta m_{-\mathbf{q}_1-\mathbf{q}_2-\mathbf{q}_3}(t_1). \quad (2.7c)$$

The quadratic Lagrangian, iL_0 , defines the following nonzero propagators:

$$\langle \delta m_{\mathbf{q}}(t) \tilde{\Psi}_{\mathbf{q}'}(t') \rangle = i(2\pi)^d \delta(\mathbf{q} + \mathbf{q}') G_{\mathbf{q}}^{(0)}(t, t') \\ = (2\pi)^d \delta(\mathbf{q} + \mathbf{q}') \theta(t - t') \exp \left[-\lambda \int_{t'}^t dt_1 [q^2 + \tau(t_1) + \frac{1}{2}um^2(t_1)] \right], \quad (2.8a)$$

$$\langle \tilde{\Psi}_{\mathbf{q}}(t) \delta m_{\mathbf{q}'}(t') \rangle = i(2\pi)^d \delta(\mathbf{q} + \mathbf{q}') G_{\mathbf{q}}^{(0)\dagger}(t, t') \\ = (2\pi)^d \delta(\mathbf{q} + \mathbf{q}') \theta(t' - t) \exp \left[\lambda \int_t^{t'} dt_1 [q^2 + \tau(t_1) + \frac{1}{2}um^2(t_1)] \right], \quad (2.8b)$$

and

$$\langle \delta m_{\mathbf{q}}(t) \delta m_{\mathbf{q}'}(t') \rangle = (2\pi)^d \delta(\mathbf{q} + \mathbf{q}') S_{\mathbf{q}}^{(0)}(t, t') = (2\pi)^d \delta(\mathbf{q} + \mathbf{q}') 2\lambda \int_{-\infty}^{\infty} dt'' G_{\mathbf{q}}^{(0)}(t, t'') G_{\mathbf{q}'}(t', t''), \quad (2.8c)$$

where the superscripts “0” and “†” denote averages in the zeroth-order theory and Hermitian conjugation, respectively.

Vertex functions are calculated in a loop expansion. As is well known, fluctuation corrections to the mean-field expressions introduce infrared divergences for $d < 4$.²³ In particular, the diagram in Fig. 1(a), which contributes to the equation of motion of $m(t)$, and the diagrams in Fig. 1(b), which contribute to the vertex function $\Gamma^{(1,1)}$, diverge for $d < 4$. We shall regularize the theory by di-

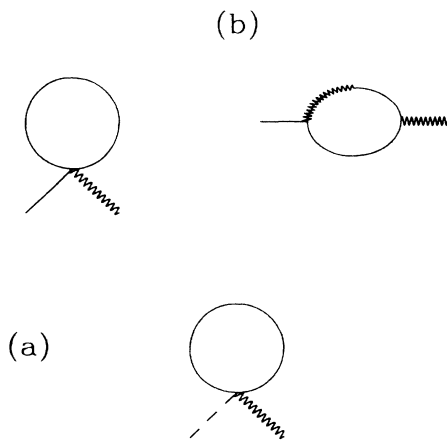


FIG. 1. (a) One-loop diagram for the equation of motion. The solid line is a dressed correlation function line, and the dashed line corresponds to a factor of $\langle m(t) \rangle$. (b) One-loop diagrams for $\Gamma^{(1,1)}$. The cubic vertices correspond to factors of $u \langle m(t) \rangle$, and the line segment corresponds to a dressed propagator.

dimensional regularization about $d=4$ and eliminate ϵ^{-1} ($\epsilon \equiv 4-d$) poles in minimal subtraction.²⁴

Terms that diverge as Λ^2 , where Λ is an upper momentum cutoff, are subtracted by additively shifting the bare temperature. The ϵ^{-1} are eliminated by multiplicatively renormalizing bare parameters (renormalized quantities are denoted by subscripts “R”) according to²³

$$u = \frac{(2\pi)^d}{S_d} u_R \left[1 + \frac{3\tilde{u}_R}{2\epsilon} \right] \quad (2.9a)$$

and

$$\tau = \tau_R \left[1 + \frac{\tilde{u}_R}{2\epsilon} \right], \quad (2.9b)$$

with

$$\tilde{u}_R \equiv \kappa^{-\epsilon} u_R, \quad (2.9c)$$

where κ is a quantity with dimension of inverse length that was introduced in the process of dimensional regularization. Since the coupling constant was redefined to absorb various angular factors [$S_d \equiv 2\pi^{d/2} \Gamma(d/2)^{-1}$ is the area of a d -dimensional sphere], m and \tilde{h} shall also be rescaled by a factor of $S_d^{1/2} (2\pi)^{-d/2}$. Moreover, to one-loop order there is no wave-function renormalization ($m = m_R$), and the Onsager kinetic coefficient does not renormalize ($\lambda = \lambda_R$).^{22(a)}

The one-loop equation of motion is obtained by evaluating the diagram in Fig. 1(a). The ϵ^{-1} poles, which arise from short-time behavior, are eliminated upon replacing bare by renormalized quantities according to Eqs. (2.9) in an ϵ expansion. The resulting one-loop renormalized equation of motion for the average order parameter becomes

$$\partial_1 m(t) + \lambda m(t)(\tau_R + \frac{1}{6}u_R m^2(t) - \frac{1}{4}\bar{u}_R \{x(t)[q_1(t) + \gamma] + q_2(t)\} + O(\epsilon^2)) = \lambda \tilde{h}(t), \quad (2.10a)$$

with

$$q_1(t) \equiv 2\lambda \int_0^\infty ds \ln(2\lambda\kappa^2 s) x(t-s) \exp\left[-2\lambda \int_0^s ds_1 x(t-s_1)\right], \quad (2.10b)$$

and

$$q_2(t) \equiv \int_0^\infty \frac{ds}{s} (2\lambda\kappa^2 s)^{\epsilon/2} [x(t-s) - x(t)] \exp\left[-2\lambda \int_0^s ds_1 x(t-s_1)\right] = \frac{1}{2\lambda} \frac{dq_1(t)}{dt} + O(\epsilon), \quad (2.10c)$$

where the tree, renormalized inverse susceptibility is defined to be

$$x(t) \equiv \tau_R + \frac{1}{2}u_R m^2(t), \quad (2.10d)$$

and γ is Euler's constant. In deriving Eq. (2.10a), repeated integrations by parts were used to separate the one-loop term into two parts: a term that for a time-independent state reproduces the one-loop contribution to the equilibrium equation of state, $q_1(t)$, and a term that is intrinsically time dependent, $q_2(t)$, and vanishes for a time-independent state. Moreover, the former term was ϵ expanded to eliminate the ϵ^{-1} poles, whereas the latter was not.²⁶ Since static renormalizations, which multiply terms local in time, suffice to make the equation of motion finite, it is *not* necessary to ϵ expand the second term (for a more complete discussion see Appendix A). The renormalized equation of motion differs from that reported in Ref. 22(c) because the subtractions differ.

It is worth noting that the one-loop correction introduces a memory term making the equation of motion non-Markovian; the significance of the memory term for various quenches will be discussed in Sec. IV. Furthermore, even though the expansion was carried out about a spatially uniform state, $m(t)$, the one-loop term includes the integrated contributions of fluctuations of arbitrary wave vectors. For a time-independent state, note that the right-hand side of Eq. (2.10a) reduces to the usual perturbative expression for the equation of state.²³ A similar calculation for the one-loop renormalized response function, with $m(t) = 0$, is given in Appendix B.

Finally, note that the units for the problem were chosen such that the coefficient of the $|\nabla\Psi|^2$ in the free energy, cf. Eq. (2.1d), was $\frac{1}{2}$. As is usually the case, and as will be shown in the next section, the units in the renormalized theory are all scaled by κ . If the true range of the interaction is increased, κ will decrease; this has the effect of reducing \bar{u}_R , cf. Eq. (2.9c), thereby making the nonlinear fluctuation terms less important and the calculation more mean-field-like.

III. RENORMALIZATION-GROUP EQUATION AND MATCH CONDITION

The renormalized quantities presented in the preceding section depend on the parameter κ introduced in the dimensional regularization of divergent one-loop integrals. The requirement that the bare theory be invariant with respect to changes of κ leads to the renormalization-

group equation for the renormalized vertex functions, $\Gamma^{(i,j)}(\{\mathbf{r}, t\}_i; \{\mathbf{r}', t'\}_j)$. As is well known, the renormalization-group equation determines the scaling properties of the vertex functions under length scale transformations. Specifically, the renormalization-group equation for the instantaneous external field \tilde{h} expressed in terms of dimensionless variables $\tilde{\tau}_R \equiv \tau_R \kappa^{-2}$, $\tilde{m}_R \equiv m_R \kappa^{-1+\epsilon/2}$, $\tilde{\lambda}_R \equiv \lambda_R \kappa^2$, and \bar{u}_R becomes

$$\left[\kappa \frac{\partial}{\partial \kappa} + \beta_\lambda \frac{\partial}{\partial \tilde{\lambda}_R} + \beta_u \frac{\partial}{\partial \bar{u}_R} + \beta_{\tau^*} \frac{\delta}{\delta \tilde{\tau}_R} + \beta_{m^*} \frac{\delta}{\delta \tilde{m}_R} + \gamma_h \right] \times \tilde{h}[\bar{u}_R, \tilde{\lambda}_R, \kappa, t; \tilde{\tau}_R(\mathbf{r}', t'), \tilde{m}_R(\mathbf{r}', t')] = 0, \quad (3.1)$$

where the one-loop Wilson functions are

$$\beta_u \equiv \kappa \frac{\partial \bar{u}_R}{\partial \kappa} \Big|_B = -\bar{u}_R (\epsilon - \frac{1}{2}\bar{u}_R), \quad (3.2a)$$

$$\beta_\tau \equiv \kappa \frac{\partial \tilde{\tau}_R}{\partial \kappa} \Big|_B = -\tilde{\tau}_R (2 - \frac{1}{2}\bar{u}_R), \quad (3.2b)$$

$$\beta_m \equiv \kappa \frac{\partial \tilde{m}_R}{\partial \kappa} \Big|_B = -\tilde{m}_R (1 - (\epsilon/2)), \quad (3.2c)$$

$$\beta_\lambda \equiv \kappa \frac{\partial \tilde{\lambda}_R}{\partial \kappa} \Big|_B = 2\tilde{\lambda}_R, \quad (3.2d)$$

$$\gamma_h \equiv -\frac{1}{2} \frac{\partial \ln(Z_\Psi)}{\partial \kappa} \Big|_B = 0, \quad (3.2e)$$

Z_Ψ is the wave function renormalization (which is one to one-loop order), and $*$ denotes integration over space and time. [Note that since the renormalization-group equation was derived by requiring that the bare theory be independent of changes in κ , the derivatives in Eqs. (3.2) are taken keeping bare quantities fixed.]

The renormalization-group equation, by incorporating information about anomalous dimensions, imposes constraints on the functional dependence of the vertex functions on their arguments. Namely, a vertex function exactly solves the renormalization-group equation when expressed in terms of the constants of motion arising from the characteristic equations associated with Eqs. (3.1)–(3.2). The exact solutions of these equations are

$$U(\kappa) \equiv \bar{u}_R \kappa^\epsilon \left[1 + \frac{\bar{u}_R}{u^*} (\kappa^\epsilon - 1) \right]^{-1}, \quad (3.3a)$$

$$T(\kappa) \equiv \tilde{\tau}_R(t) \kappa^2 \left[1 + \frac{\tilde{u}_R}{u^*} (\kappa^\epsilon - 1) \right]^{-1/3}, \quad (3.3b)$$

$$M(\kappa) \equiv \tilde{m}_R(t) \kappa^{1-\epsilon/2}, \quad (3.3c)$$

and

$$\Lambda(\kappa) \equiv \tilde{\lambda}_R \kappa^{-2}, \quad (3.3d)$$

where $u^* \equiv 2\epsilon/3$ is the value of the coupling constant at the nontrivial fixed point.

Therefore, a vertex function becomes consistent with the renormalization-group equation (and it is written in a

form appropriate for the study of crossover effects) by writing it in terms of the functions defined by Eqs. (3.3) and by ϵ expanding the difference. In addition, naive dimensional analysis must be satisfied, i.e., vertex functions must transform according to their canonical dimensions under a length scale transformation $\kappa \rightarrow \kappa\rho$. [Note that by expressing m_R and λ_R in terms of the corresponding dimensionless variables, naive dimensional analysis is trivially satisfied upon solving the renormalization-group equation, cf. Eqs. (3.3c) and (3.3d)].

In particular, upon rescaling the equation of motion for $m(t)$ by a time-dependent $\rho(t)$, the one-loop, crossover form of the equation of motion becomes

$$\begin{aligned} \rho^{1-\epsilon/2}(t) \partial_t m(t) &= \Lambda(t) \rho^{3-\epsilon/2}(t) \tilde{h}(t) - M(t) \Lambda(t) [T(t) + \frac{1}{6} U(t) M^2(t)] \\ &\quad + \frac{1}{4} M(t) U(t) \{ \Lambda(t) X(t) [Q_1(t) + \gamma] + Q_2(t) \} + O(\epsilon^2), \end{aligned} \quad (3.4a)$$

with

$$Q_1(t) \equiv 2 \int_0^\infty ds \ln[2\Lambda(t)s] \Lambda(t-s) X(t-s) \exp \left[-2 \int_0^s ds_1 \Lambda(t-s_1) X(t-s_1) \right], \quad (3.4b)$$

and

$$Q_2(t) \equiv [2\Lambda(t)]^{\epsilon/2} \int_0^\infty \frac{ds}{s} s^{\epsilon/2} [\Lambda(t-s) X(t-s) - \Lambda(t) X(t)] \exp \left[-2 \int_0^s ds_1 \Lambda(t-s_1) X(t-s_1) \right], \quad (3.4c)$$

where

$$X(t) \equiv T(t) + \frac{1}{2} U(t) M^2(t), \quad (3.4d)$$

and $3-\epsilon/2$ is the canonical dimension of \tilde{h} . To simplify notation the explicit $\kappa\rho$ dependence of the constants of motion, Eqs. (3.3), was dropped. In addition, note that the logarithm in Eq. (3.4b) provides the necessary $\ln[\kappa\rho(t)]$ terms to convert the perturbative expression, cf. Eqs. (2.10), into crossover form. Moreover, as discussed in Ref. 22(c), the derivative term does not act on the scale parameter. The memory term, however, is scaled by $\rho(t-s)$; since it arises from the time convolution of two propagators [cf. Fig. 1(a)], a time-local rescaling of the propagators results in the nonlocal rescaling shown in Eqs. (3.4b) and (3.4c).²⁷

As in static critical phenomena, the scale parameter is linked to average thermodynamic variables by the match condition, which for dynamic phenomena may be time dependent. In effect, the match condition resums the perturbation series and may be used to eliminate logarithmic singularities that are generated by the ϵ expansion. Previously,^{22(c)} it was specified by imposing a time-dependent generalization of the match condition used by Brézin *et al.*²⁸ by requiring that $M^2(t)=1$. This match condition, however, becomes meaningless for $m=0$, and its static version does not exponentiate the explicit logarithmic singularity in the equation of state.

In a static calculation, a more appropriate match condition is obtained by requiring that the one-loop terms in the equation of motion do not introduce logarithmic singularities close to the critical point, thereby ensuring

that the perturbation series remain valid. This argument was initially used by Rudnick and Nelson¹⁸ in the derivation of the equation of state in the critical region. In particular, logarithmic singularities in the equation of state were exponentiated uniformly by linking the scale parameter to the tree inverse susceptibility via

$$X_{\text{eq}} \equiv T_{\text{eq}} + \frac{1}{2} U M_{\text{eq}}^2 = 1, \quad (3.5a)$$

where the subscript “eq” denotes equilibrium values.

In the dynamic theory, cf. Eq. (3.4a), there are no explicit logarithmic singularities. It is easy to show, however, that they are obtained from $Q_1(t) + \gamma$ in the static limit. Therefore, a possible time-dependent generalization of the static Rudnick-Nelson match condition, which for a time-independent state reduces to Eq. (3.5a), is

$$Q_1(t) + \gamma = 0, \quad (3.5b)$$

and $Q_1(t)$ was defined by Eq. (3.4b). [Another time-dependent match condition $X(t)=1$ cannot be used in the unstable region where the susceptibility is negative.]

As discussed in I, the Rudnick-Nelson equation of state exhibits unphysical behavior inside the coexistence curve. For that reason an ϵ -dependent modification of Eq. (3.5a) was proposed. Specifically, it was suggested that the tree inverse susceptibility in the match condition be replaced by a naively exponentiated, approximate form of the one-loop inverse susceptibility.

The corresponding time-dependent generalization of the new match condition becomes Eq. (3.5b), where $X(t)$ is replaced by

$$X_\beta(t) \equiv T(t) \left[\frac{\alpha + U(t)T^2(t)}{\alpha + U(t)} \right]^{-[\beta(t)-1/2]/2} + \frac{1}{2}U(t)M^2(t) \left[\frac{\alpha + U(t)T^2(t)}{\alpha + U(t)} \right]^{-3[\beta(t)-1/2]/2}, \quad (3.6a)$$

and $\beta(t)$ is a crossover form of the order-parameter critical exponent²⁹

$$\beta(t) \equiv \frac{1}{2} - \frac{U(t)}{4 - U(t)}. \quad (3.6b)$$

The real part of the equation of state obtained in Ref. 16 is recovered in the static limit when the match condition, cf. Eq. (3.5b), with the aforementioned modification, cf. Eq. (3.6), are used in Eq. (3.7).

The time-dependent match condition makes the scale

$$\begin{aligned} \rho^{1-\epsilon/2}(t)\partial_t m(t) = & \Lambda(t)\rho^{3-\epsilon/2}\tilde{h}(t) - M(t)\Lambda(t)[T(t) + \frac{1}{6}U(t)M^2(t)] \\ & + \frac{1}{4}U(t)M(t)[2\Lambda(t)]^{\epsilon/2} \int_0^\infty \frac{ds}{s} s^{\epsilon/2} [\Lambda(t-s)X_\beta(t-s) - \Lambda(t)X_\beta(t)] \\ & \times \exp \left[-2 \int_0^s ds_1 \Lambda(t-s_1)X_\beta(t-s_1) \right] + O(\epsilon^2), \end{aligned} \quad (3.7a)$$

and

$$\frac{d \ln[\kappa\rho(t)]}{dt} = \int_0^\infty \frac{ds}{s} [\Lambda(t-s)X_\beta(t-s) - \Lambda(t)X_\beta(t)] \exp \left[-2 \int_0^s ds_1 \Lambda(t-s_1)X_\beta(t-s_1) \right] + O(\epsilon), \quad (3.7b)$$

where the $O(\epsilon)$ corrections arise from replacing X by X_β in Eq. (3.5b). Note that the equation of motion of the scale parameter is solved for any time-independent m , τ , and $\kappa\rho$; the initial condition, however, forces time-independent solutions to satisfy $X_\beta(\kappa\rho)=1$. For some quenches, our numerical solution to this integrodifferential equation is not very stable, and the original expression, cf. Eq. (3.5b), is solved instead. As before, Eqs. (3.7a) and (3.7b) reduce to the static equation of state presented in I for time-independent states. The numerical solution of Eqs. (3.7) is presented in the next section, with $\alpha=1$ in the match condition. Finally, as was mentioned in the preceding section, if the range of the interaction is increased, \tilde{u}_R decreases and the parts of $U(t)$, etc., with anomalous dimension drop out; hence, the scale parameter drops out of the calculation and mean-field theory results are obtained.

IV. RESULTS

A. Instantaneous external-field and temperature quenches

Figure 2(a) shows the time evolution of the order parameter for a system with $u/u^*=0.10$ under instantaneous external-field quenches close to the pseudospinodal; the corresponding variation of the scale parameter is presented in Fig. 2(b). Note that for quenches into the

parameter history dependent, and it ensures that Eq. (3.5b) coupled to Eqs. (3.6) have real, nonperturbative solutions even for instantaneous quenches into the unstable region. Roughly speaking, the time integrals will have contributions from the entire time interval during which the susceptibility is negative; the convergence of the integrals is ensured by starting the quench from a stable region. Moreover, as in the static case, the match condition introduces a second length scale, independent of the correlation length ξ , which, in a static calculation, diverges along a line of ϕ^4 critical points, which we call the universal spinodal (assuming that the system could be forced to remain there).¹⁶

For some quenches, a computationally more efficient form of Eqs. (3.4)–(3.6) is obtained by differentiating the match condition, Eq. (3.5), with respect to time to get a set of two coupled integrodifferential equations for the average order parameter and the scale parameter,

unstable region the system reaches the final equilibrium state, whereas for quenches into the metastable region the system remains trapped in the local minimum. As mentioned in the Introduction, this is a consequence of our neglecting fluctuations which lead to nucleation (e.g., droplets) and cause metastable states to decay.

For quenches into the unstable region the time-dependence of the scale parameter—which is a coherence length of critical-like fluctuations—is noteworthy: initially it follows the changing order parameter until the system reaches the universal spinodal region, whereupon it starts increasing rapidly. It attains its equilibrium value by decreasing abruptly when the system leaves the universal spinodal region. The rapid changes of the scale parameter are triggered by changes in $m(t)$ and arise because the instantaneous modified susceptibility X_β is negative, cf. Eq. (3.7b).

When the scale parameter becomes large the zero- and one-loop terms vanish; hence, the time evolution of the order parameter simplifies, and the rate of change is proportional to $\tilde{h}(t)$, as is evident from the linear part in the time evolution of the order parameter; cf. Figs. 2 and 3. Indeed, once the scale parameter has become sufficiently large, its role in the dynamics drops out, since the zero- and one-loop terms vanish. This is fortunate, since when the scale parameter is extremely large, its evolution changes in a number of significant ways depending on the

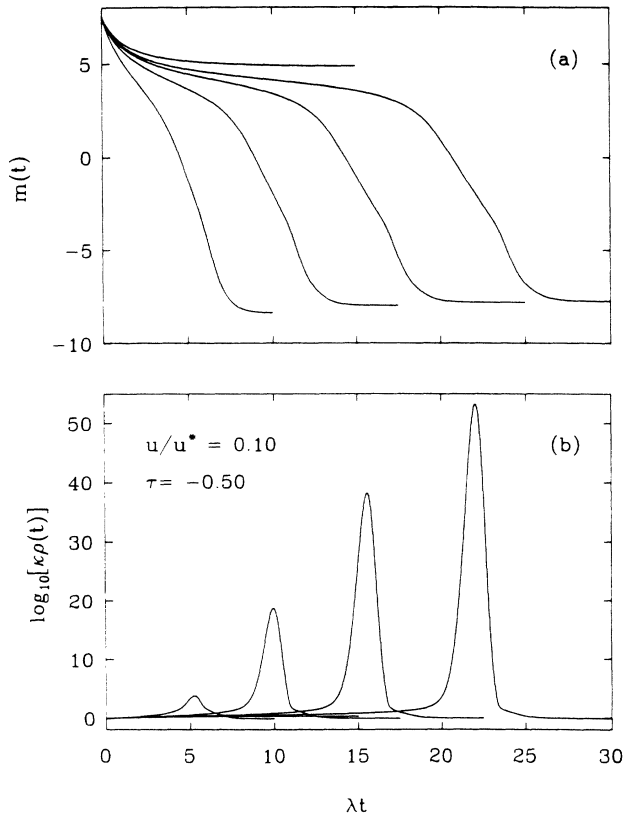


FIG. 2. (a) Time evolution of the order parameter under instantaneous, isothermal, external-field quenches for $u/u^* = 0.10$, $\tau_f = -0.50$, and $\tilde{h}_i = 1.00$. The ratios of the external field to the static spinodal field, $h^* \equiv \tilde{h}/\tilde{h}_{sp}$, are 0.93, 1.09, 1.16, 1.35, and 1.94, reading from top to bottom. (b) The corresponding variation of the logarithm of the scale parameter $\rho(t)$ which increases as the spinodal is approached from the unstable region.

choice of match condition and on the details of the ϵ expansion.

Similar behavior is observed for $u/u^* = 1.0$, as shown in Figs. 3(a) and 3(b). Note, however, that the decay of the order parameter is nonmonotonic; there is a small loop in $m(t)$ before it reaches its final equilibrium value. This behavior, in contrast with that of mean-field theory (which is monotonic), is a consequence of the non-Markovian character of the equation of motion. Specifically, the order parameter remains in local equilibrium with the instantaneous free-energy surface, which, however, differs from the quasistatic surface because of $\rho(t)$. Since the instantaneous free energy depends on the nonequilibrium scale parameter, which is larger than its quasistatic value, it is easy to show that $m(t)$ scales as $[\rho(t)/\rho_{eq}]^{1/\nu-2}$ in the critical region, where $\nu \sim (2-\epsilon/3)^{-1}$ is the usual correlation-length exponent in equilibrium. The loop disappears upon replotting the data given in Fig. 3(a) as a function of $m(t)\rho^{-\epsilon/3}(t)$.

The significance of the scale parameter and its effect on the apparent pseudospinodal can be examined by considering combined external-field and temperature quenches. Since the quasistatic equation of state¹⁶ is cubic in m , the

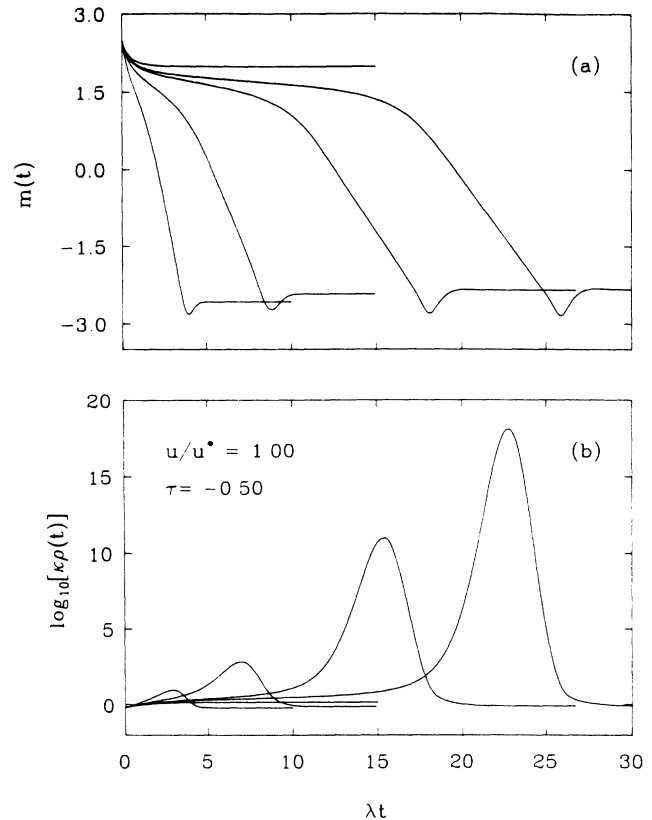


FIG. 3. (a) and (b) panels are as in Fig. 2 for $u/u^* = 1.00$. The reduced external fields, h^* , are 0.73, 1.10, 1.22, 1.83, and 3.66, reading from top to bottom. Note that the late-time decay of the order parameter becomes monotonic upon replotting the data as a function of $m(t)\rho^{-1/3}(t)$.

analysis of the regions of attraction of the metastable and absolute free-energy minima is similar to the mean-field analysis.⁵ The equation of motion may be written as

$$\partial_t m(t) \propto -[m(t) - m_+(\rho(t))][m(t) - m_0(\rho(t))] \times [m(t) - m_-(\rho(t))]. \quad (4.1)$$

where $m_- \leq m_0 \leq m_+$, and where factors of $\kappa\rho$ that arise from canonical dimensional analysis were canceled. The three roots will be real for final temperature, τ_f , below the critical temperature and for final external field, \tilde{h} , will be less than zero but greater than the value at the pseudospinodal.

In the mean-field approximation, the roots do not change in time and the evolution is governed solely by the final-state free-energy surface. Consequently, states with initial magnetization $m_i > m_0$ monotonically approach the metastable minimum, and states with $m_i < m_0$ decay to the absolute minimum, m_- .

In the present calculation the external parameters \tilde{h} and τ_f are assumed to change instantaneously, but the order and scale parameters do not. Thus, the free energy that governs the initial dynamics is determined by \tilde{h} , τ_f , and the initial scale parameter ρ_i . The new bifurcation point, $m_0(\rho_i)$, becomes a function of the initial scale pa-

parameter and is displaced with respect to the bifurcation point obtained from the adiabatic free-energy surface, $m_0(\rho_{\text{eq}})$ (where ρ_{eq} is the scale parameter at the pseudospinodal).

For quenches from the critical isotherm at $u = u^*$ it can be shown that the shift of the bifurcation point is related to the ratio ρ_i/ρ_{eq} ; if the ratio is less than one, then the region of initial attraction to the metastable minimum increases and vice versa. Since ρ is a measure of the strength of fluctuations, a smaller value of ρ implies that the system has smaller amplitude fluctuations than those in a quasistatic quench and hence, initially, appears somewhat more stable.

For the quenches from the critical isotherm, the ratio of the scale parameters is always less than one; i.e., the coherence length of fluctuations at the unstable root is greater than the coherence length at the initial state. Hence, as is confirmed by our numerical work, the region of initial values of the magnetization that are attracted to the metastable minimum is larger than the region predicted from a naive analysis of the static one-loop free energy.

In addition, memory effects become important as the system evolves. Their effect is more pronounced under quenches where the initial magnetization is close to the bifurcation point m_0 . We show such a quench in Figs. 4(a) and 4(b). Initially the order parameter has positive slope and tends towards the metastable minimum, as a quasistatic analysis would predict. During the quench, however, changes of the nonequilibrium scale parameter significantly modify the free energy and the order parameter decays to the final true equilibrium state. Hence, under some quenches, even though the initial dynamics may be described by a suitably chosen quasistatic free energy, the full-time evolution is not.

In summary, we see that in the critical region, the dynamics can be qualitatively different than that predicted by mean-field theory. Memory effects, at least in as much as they determine the scale parameter, become important. Nonetheless, analyses based upon quasistatic free-energy surfaces evaluated at the instantaneous scale parameter can be used to predict qualitative features of either the initial- or final-stage dynamics.

B. Instantaneous critical quenches

The primary quantity of interest for critical quenches is the equal-time structure factor. For a nonconserved

$$S_q(t) = 2\lambda \exp(-2\lambda q^2 t) \int_{-\infty}^t dt_1 \exp \left[2\lambda q^2 t_1 - 2 \int_{t_1}^t dt_2 \left[\Lambda(t_2) T(t_2) - \frac{1}{4} U(t_2) Q_2(t_2) \right] \right], \quad (4.3a)$$

where $Q_2(t)$ was defined by Eq. (3.4c), with $T(t)$ replacing $X(t)$. Furthermore, it is evident from Eqs. (4.2) and (B3) that the structure factor satisfies the differential equation

$$\partial_t S_q(t) = -2 \left[\lambda q^2 + \Lambda(t) T(t) - \frac{1}{4} U(t) Q_2(t) \right] S_q(t) + 2\lambda. \quad (4.3b)$$

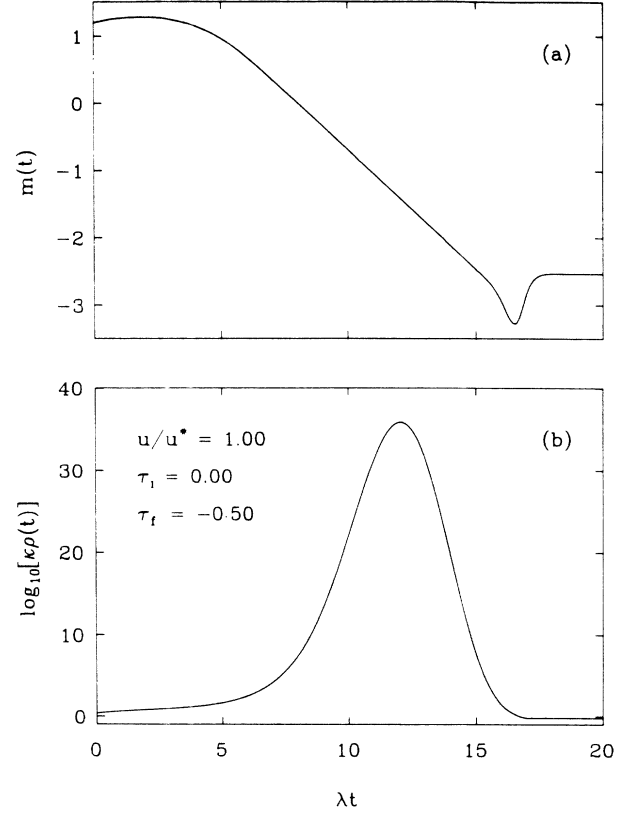


FIG. 4. (a) and (b) panels are as in Fig. 2. The order parameter initially has positive slope, as the preceding quasistatic analysis based on $\rho_i(t)$ would predict, but the solution of the full, one-loop, dynamical equation of motion shows that the order parameter decays to the final equilibrium state. The parameters of the quench are $u/u^* = 1.00$, $\tau_i = 0.00$, $\tau_f = -0.50$, $\tilde{h}_i = 1.00$, and $\tilde{h}_f = -0.075$.

order parameter, its second moment, or, alternatively, the maximum of $q^2 S_q(t)$, has been identified with the inverse average domain size.¹³ To one-loop order, the structure factor is given by

$$S_q(t, t') = 2\lambda \int_{-\infty}^{\infty} dt_1 G_q(t, t_1) G_{-q}(t', t_1). \quad (4.2)$$

Substituting the renormalized, one-loop, crossover form of the Green's function [cf. Eq. (B3)], we obtain the equal-time structure factor

Under critical quenches the scale parameter increases without bound; its time dependence under a series of quenches from a noncritical initial state is shown in Fig. 5. The growth law for the scale parameter does not satisfy a simple scaling law. Under instantaneous quenches close to the critical point, however, it is easy to show that Eq. (3.7b) becomes

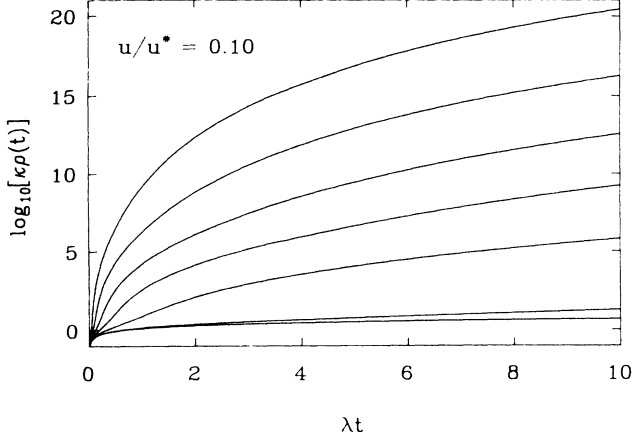


FIG. 5. The logarithm of the scale parameter under a series of instantaneous temperature quenches at zero external field: $u/u^* = 0.10$ and $\tau_i = 100.0$. The final temperatures are -20.00 , -10.00 , -5.00 , -2.50 , -1.00 , -0.10 , and -0.01 , reading from top to bottom.

$$\frac{d \ln[\kappa\rho(t)]}{dt} = \Lambda_i T_i e^{2\Lambda_i T_i t} E_1(2\Lambda_i T_i t) + O\left(\frac{\tau_f}{\tau_i}\right), \quad (4.4)$$

where the subscript “ i ” denotes the initial equilibrium values at the initial reduced temperature τ_i , τ_f is the final temperature, and $E_1(z)$ is the exponential integral function. By using the asymptotic expansion for $E_1(z)$ it follows that the scale parameter increases as $\kappa\rho(t) \propto t^{1/2}$, a behavior that is consistent with previous analyses of non-linear relaxation of the order parameter close to the critical point.^{22(c)} This growth law, however, is only transient if the final temperature is not exactly equal to the critical temperature; the scale parameter eventually crosses over to the more complicated time dependence shown in Fig. 5.

The unbounded increase of the scale parameter forces the zero- and one-loop terms in the equation of motion of the structure factor to vanish at late times. Consequently, three distinct time regimes may be distinguished: early, intermediate, and late times. There should be a fourth time regime, but this is not seen in the present calculation (see the following).

At early times, the scale parameter is small, and the dynamics is described by the mean-field theory. Specifically, in the mean-field limit, cf. Eq. (4.3a), the well-known analysis gives

$$S_q(t) = \frac{1}{q^2 + \tau_f} + \frac{(\tau_f - \tau_i) e^{-2\lambda(\tau_f + q^2)t}}{(\tau_f + q^2)(\tau_i + q^2)} \quad (4.5)$$

for $t \geq 0$. Since here $\tau_f < 0$, the mean-field approximation implies exponential growth for sufficiently small q .

Deviations from the mean-field approximation set in with the growth of the scale parameter. From Eqs. (3.3a)–(3.3d) and (4.3a), it follows that the crossover from mean-field behavior will occur when

$$\kappa\rho(t) \sim \left[\frac{u^*}{\tilde{u}_R} - 1 \right]^{1/\epsilon}. \quad (4.6)$$

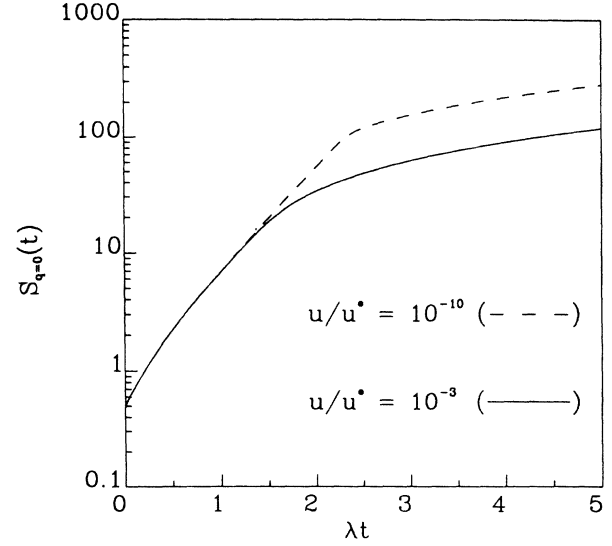


FIG. 6. The $q=0$ value of the structure factor as a function of the coupling constant for critical quenches (also see Fig. 7). Here, $\tau_i = 1.0$ and $\tau_f = -1.0$.

The existence of the mean-field, exponential-growth region is confirmed numerically as shown in Fig. 6. Note, that, as expected, the short-time region is larger when \tilde{u}_R is smaller. Conversely, if \tilde{u}_R/u^* is not sufficiently small, then it may not be possible to clearly identify a region of exponential growth.

At late times, the equation of motion of $S_q(t)$ reduces to the mean-field equation for a quench to the critical temperature; the system becomes effectively critical, without acquiring, however, nonclassical exponents (at least in a one-loop calculation). The crossover occurs when $\lambda q^2 \sim \Lambda(t)T(t)$, cf. Eq. (4.3b). In this case, the structure factor may be written as

$$S_q(t) \sim \frac{e^{-2\lambda q^2 t}}{q^2 + \tau_i^*} + \frac{1}{q^2} (1 - e^{-2\lambda q^2 t}), \quad (4.7)$$

where τ_i^* is an effective initial temperature. At $q=0$, $S_{q=0}(t) \sim (\tau_i^*)^{-1} + 2\lambda t$, cf. Eq. (4.7), in sharp contrast with the exponential growth predicted in the mean field [cf. Eq. (4.5)]. This is shown in Fig. 7, where the late-time linear behavior is clear. Mazenko *et al.* also predict nonexponential growth of the structure factor, although with a different exponent. Moreover, as obtained by Binder *et al.*, the dynamics is diffusive, with a characteristic length, $L(t)$, growing as $L(t) \sim (2\lambda t)^{1/2}$. In addition, the structure factor decays as q^{-2} as $q \rightarrow \infty$.

In order to study the intermediate time dependence of the structure factor, we write

$$S_q(t) \equiv \frac{e^{-2\lambda q^2 t}}{q^2 + \tau_i^*} + \frac{1}{q^2} (1 - e^{-2\lambda q^2 t}) + B(t)F(q, t). \quad (4.8)$$

The intermediate time behavior is described by the last term in Eq. (4.8). We found that the function $B(t)F(q, t)$ has a maximum at $q_F(t)$, which approaches zero as time increases, and that its value at the maximum first increases but ultimately decreases.³⁰ Upon rescaling q by

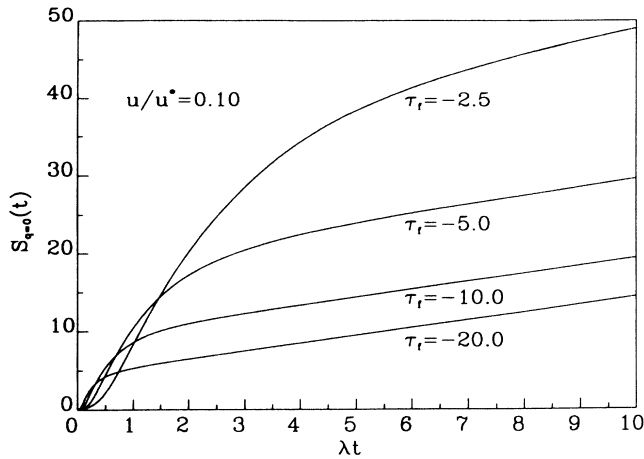


FIG. 7. The structure factor at $q=0$ under instantaneous temperature quenches with $u/u^*=0.10$ and $\tau_i=100.0$.

$q_F(t)$ and normalizing the function at its maximum, the resulting function, i.e.,

$$\tilde{S}_n[q/q_F(t)] \equiv \frac{F(q,t)}{F[q_F(t),t]}, \quad (4.9)$$

admits, at least approximately, a scaling form at late times. In Fig. 8 we show $\tilde{S}_n(x)$ for a series of different times during the same quench; as time increases a universal scaling function is approached. For the data shown in Fig. 8, the amplitude $B(t)$, which is shown in Fig. 9, decays as $\exp[-0.56(\lambda t)^{1/2}]$ at long times; this behavior is similar to that observed by Billotet and Binder¹³, although the characteristic size, $q_F^{-1}(t)$, corresponding to this component does not grow like $t^{1/2}$ except at very short times, unlike the case in Ref. 13. The scaling function, $\tilde{S}_n(x)$, is approximately Gaussian near the peak, but

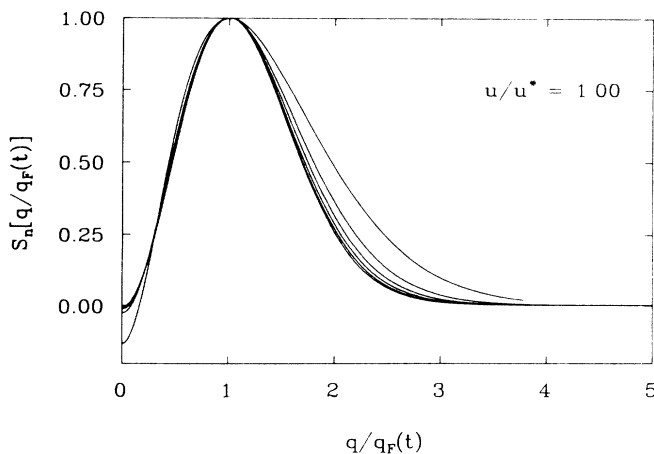


FIG. 8. The normalized function that gives the intermediate-time contribution to the structure factor, $\tilde{S}_n(x)$ (late-time behavior has been subtracted) from $S_q(t)$. The curves are parametrized by time: 0.40, 1.20, 2.00, 2.80, 3.60, and 4.40, reading from right to left. Note that an approximate scaling function is approached as time increases. The parameters of the quench are as follows: $\tau_i=100.0$, $\tau_f=-5.00$; $u/u^*=1.00$. In addition, $\tau_i^*=0.19518$.

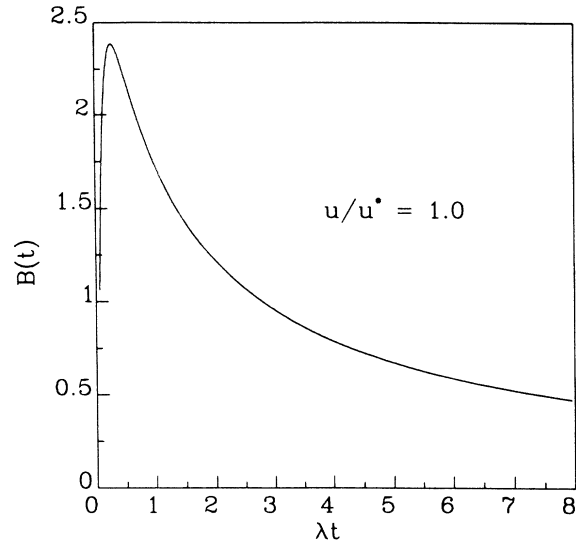


FIG. 9. The amplitude of the intermediate-time component for the case shown in Fig. 8

ultimately decays as $x^{-\alpha}$, with $\alpha \approx 4$, as $x \rightarrow \infty$. This form is functionally similar to that found by Mazenko *et al.*, although we stress that this component disappears at long times.

As was mentioned earlier, the crossover time from intermediate- to late-time behavior is determined by $\lambda q^2 \sim \Lambda(t)T(t)$; cf. Eq. (4.3b). This suggests, cf. Eq. (3.3b), that $q_F(t) \sim |\tau_f|^{1/2} [\kappa\rho(t)]^{1/(2\nu)-1}$, where $1/(2\nu) - 1 \sim -\epsilon/6$. In Fig. 10 we show q_{\max} [defined as the maximum of $q^2 S_q(t)$] and $q_F(t)$ as functions of the scale parameter; the three time regimes are clearly observed for $u/u^*=0.10$, whereas for $u/u^*=1.0$ only intermediate- and late-time behavior is seen. The crossover from the short-time behavior is in accord with Eq. (4.6). When the scale parameter is large, $q_{\max}(t)$ and $q_F(t)$ are proportional to $[\kappa\rho(t)]^{-\epsilon/6}$, as predicted.

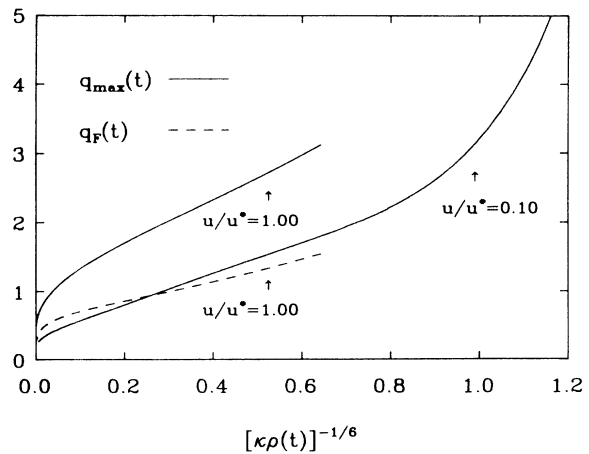


FIG. 10. The maximum of $q^2 S_q(t)$, q_{\max} (solid line), and $q_F(t)$ (dashed line) as functions of $[\kappa\rho(t)]^{-1/6}$. Two time regimes are observed for $u/u^*=1.0$ and three for $u/u^*=0.1$. Note the linear (intermediate-time) region. For $u/u^*=1.00$ the final temperature is -20.00 , and for $u/u^*=0.10$ it is -5.00 . For all cases $\tau_i=100.00$.

The current calculation exhibits only the three time domains already discussed; a last time region, one not seen here, should correspond to interfacial growth. In critical quenches, this should have diffusive dynamics and satisfy the Debye-Porod law; i.e., the structure factor should decay as $q^{-(d+1)}$.

V. DISCUSSION AND CONCLUSIONS

We have presented a one-loop, renormalized, non-Markovian equation of motion for the average order parameter of a time-dependent Landau-Ginzburg model with nonconserved order parameter (model *A* of the critical dynamics²⁰) and numerically solved it for various quenches into the unstable region.

A second length scale, the scale parameter, introduced by a dynamic generalization of our previously presented match condition,¹⁶ was found to influence the dynamics in a number of important ways (e.g., nonmonotonic order-parameter relaxation, diffusive critical dynamics, etc.).

The scale parameter is a measure of the volume where nonlinear interactions, similar to those found at the critical point, are large. When the scale parameter is large, the system behaves as if it were at the critical temperature, with zero magnetization, in the presence of an external field [cf. Sec. IV(A)]. The scale parameter does not respond instantaneously to the changes in temperature, field, and magnetization, and this is responsible for the relaxation being nonmonotonic, the effect becoming more pronounced the more the scale parameter's evolution lags behind that of the order parameter. Moreover, the extent of these effects is determined by the size of the coupling constant and by the ratio of the scale parameter to its value on the adiabatic free-energy surface, and many of the scaling laws and qualitative features of the present calculation can be deduced by considering a mean-field free-energy surface evaluated at the appropriate (e.g., initial) value of the scale parameter.

The universal spinodal region, which is bounded by the lines along which the scale parameter diverges in a static calculation, is a region of dramatic increase of the scale parameter. The scale parameter can become extremely large in noncritical quenches. In this case, its growth law is nontrivial, and the higher-order terms in ϵ are likely to be important. Fortunately, once the scale parameter is sufficiently large, it effectively drops out of the calculation.

The free-energy surface that approximately governs the dynamics depends on the scale parameter. Under various quenches—which involve abrupt changes of external variables or of the scale parameter—the appropriate instantaneous free-energy surface was found to differ from the adiabatic free-energy surface evaluated at the instantaneous thermodynamic variables. Unlike previous calculations, where the time evolution is governed by a coarse-grained free energy dependent on an arbitrary coarse-graining length,^{8,9,31} our free energy depends on the scale parameter, which is determined self-consistently by a memory-dependent match condition.

For instantaneous quenches the scale parameter initial-

ly responds slowly; the initial time evolution is governed by a modified free energy that depends on the final temperature and field and the initial scale parameter. Thus, the region of attraction of the metastable state becomes diffuse and dependent on the initial state of the system and quench rate.

For critical quenches we find three distinct time regions: (1) short times, where mean-field dynamics is approximately valid and (2) intermediate times, where the structure factor develops a second component that has a scaling form. This corresponds to regions with a characteristic size that scales as $[\kappa\rho(t)]^{-\epsilon/6}$ (which does not seem to correspond to a simple power law in time). Moreover, this component of the structure factor does not continue to grow, and at long times it disappears. Finally, (3) at late times the divergent scale parameter forces the zero- and one-loop terms to vanish, the system appears critical, and the structure factor is approximately given by the mean-field structure factor for a quench from an effective initial temperature to the critical temperature.

Some of our results are similar to those obtained by other groups although they were obtained without introducing any special decompositions of the order parameter or of the reduced distribution functions; the introduction of the memory-dependent scale parameter seems to be sufficient. It must be stressed that the physical processes considered here are different than those considered before. In much of the earlier work, the bimodal character of the order-parameter fluctuations plays a key role, whereas in this work, this character was not included explicitly. What was included were fluctuation processes characteristic of the critical point. As was discussed in the Introduction, this should be reasonable near T_c , even for critical quenches, for sufficiently short times. Of course, results specific to having a strongly bimodal distribution will not be obtained, and, in particular, naive mean-field results are obtained for $d > 4$.

At least one feature of the present calculation, like many of its predecessors,¹³ is disturbing, namely, the absence of the $q^{-(d+1)}$ tail from the high- q , long-time form of the structure factor. Such a dependence is characteristic of scattering from sharp interfaces. To be sure, q^{-4} dependence is seen in the intermediate-time component; however, to some extent this results from the manner in which this component is defined (q^{-4} is the next term in an expansion in q^{-2}) and will not depend strongly on the spatial dimensionality (e.g., by including two-loop corrections associated with the exponent η). Thus the correct d dependence would not be obtained even if we considered the theory only for intermediate times, e.g., for times where the intermediate-time component is growing and where the scale parameter is not too large.

What seems most likely is that the present theories do not adequately describe the mechanism whereby interfaces sharpen. As expected, the long-time motion is diffusive, and has an algebraically (here, linearly) growing intensity. On the other hand, the interfaces should be diffuse near the critical point; hence, the domains must be much larger, and the corresponding times much longer, before Porod's law should be observed. In this case, we

expect that there should be a well-defined separation of timescales between the latest time observed here and that which gives Porod's law behavior.

Since the evolution of the instantaneous free-energy surface, as determined by the scale parameter, can lag behind the adiabatic one, the relaxation of the order parameter becomes nonmonotonic, in sharp contrast with mean-field theory. If observed experimentally, this should provide confirmation of the theory. For the effect to be observed, it is necessary that the scale parameter becomes large and that the effective nonlinear coupling constant be large enough; in general, this should happen near the critical point. Similarly, the specific predictions for critical quenches (cf. Sec. IV B) should be relatively easy to verify.

In a future work, we plan to extend our treatment of droplet fluctuations to the dynamic regime, thereby incorporating nucleation and droplets into the present calculation.

ACKNOWLEDGMENTS

We thank Martin Grant and Mark Sutton for useful discussions. A portion of this work was supported by the National Sciences and Engineering Research Council of Canada, by Le Fonds pour la Formation de Chercheurs et l'Aide à la Recherche du Québec, and by the National Science Foundation.

APPENDIX A: NUMERICAL SOLUTION OF THE EQUATION OF MOTION

The derivation of the perturbative expression for the equation of motion, Eqs. (2.10), was based on the ansatz that the intrinsically dynamic term, $q_2(t)$ defined by Eq. (2.10c), should not be ϵ expanded because it does not generate ϵ^{-1} poles. Since the static renormalization constants (which multiply terms local in time) renormalize the dynamic equation of motion to one-loop order, the ϵ^{-1} poles are canceled by terms that do not vanish for time-independent states, i.e., $q_1(t)$. Thus, the ϵ expansion of $q_2(t)$ is not necessary to cancel ϵ^{-1} poles. The kind of resummation implied by our ansatz, where some ϵ -dependent terms are not expanded, has been used previously, most notably in the analysis of the N -vector model equation of state²⁶ and in the calculation of the droplet free energy.¹⁶

Furthermore, the ansatz was suggested by the numerical solution of the ϵ -expanded equation of motion, namely by the solution of Eq. (3.7b) coupled to

$$\begin{aligned} \rho^{1-\epsilon/2}(t)\partial_t m(t) &= \Lambda(t)\rho^{3-\epsilon/2}\tilde{h}(t) \\ &\quad - M(t)\Lambda(t)[T(t) + \frac{1}{6}U(t)M^2(t)] \\ &\quad + \frac{1}{4}U(t)M(t)\frac{d\ln[\kappa\rho(t)]}{dt} + O(\epsilon^2). \end{aligned} \quad (\text{A1})$$

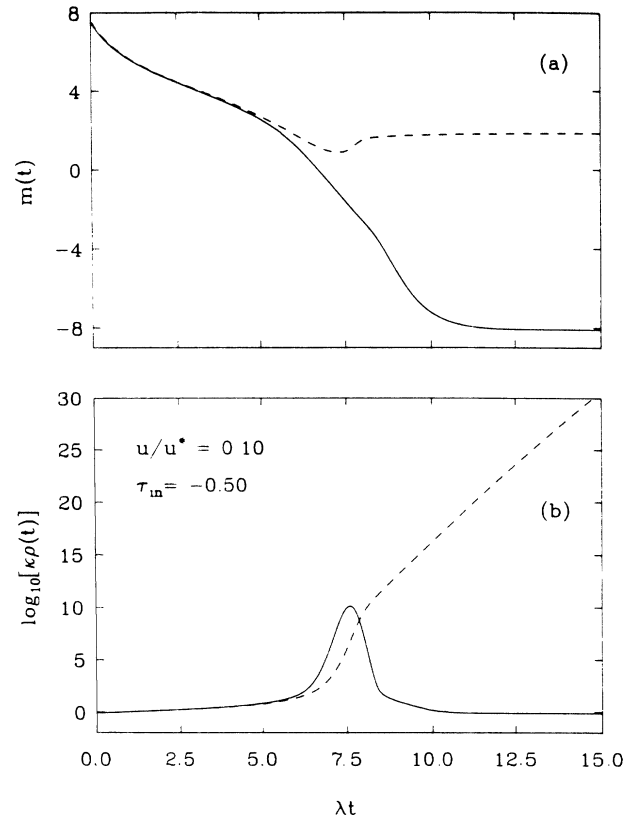


FIG. 11. (a) The solid curve is the solution of the tree order-parameter equation of motion, written in crossover form, and the dashed curve the solution of the one-loop equation of motion without exponentiating the $s^{\epsilon/2}$ term. Note that the latter curve exhibits unphysical behavior and that the system gets trapped in a metastable state that is not a solution of the static one-loop free energy, $\tilde{h} > h_{sp}$. The quench parameters are $\tau = -0.50$, $u/u^* = 0.10$, and $\tilde{h}/h_{sp} = 1.29$; (b) the logarithm of the scale parameter for the two equations discussed in (a).

We found that, for a class of quenches close to the pseudospinodal, the one-loop term dominates the zero-loop terms resulting in unexpected behavior of the order parameter. In Fig. 11 we show the time evolution of the order and scale parameters, as determined from the zero-loop equation of motion (solid line) and from the full one-loop equation of motion (dashed line). It is seen that the effect of the one-loop term is significant and cannot be treated perturbatively. We believe that this is an artifact of our approximation, i.e., of the ϵ expansion, which disappears when the ansatz is used, see Fig. 3.

Similar behavior was observed for the time-dependent generalization of the Nelson-Rudnick condition, Eq. (3.5b), and in a perturbative solution of the coupled equations. In the latter case we found that the perturbation was too large, indicating a breakdown of the expansion.

An alternative approach is to eliminate the one-loop terms by including them in the match condition. It is easily seen, however, that this is problematic because the scale parameter will diverge in regions where the susceptibility changes sign.

APPENDIX B: RESPONSE FUNCTION FOR CRITICAL QUENCHES

The equation of motion of the propagator is written as

$$\partial_t G_q(t, t_0) = -i \int_{t_0}^t dt' \Gamma_q^{(1,1)}(t, t') G_q(t', t_0), \quad (\text{B1})$$

where t_0 is the time of the perturbation and $\Gamma_q^{(1,1)}$ the ap-

propriate vertex function. [The factor of i arises from the definition of the vertex functions, cf. Eq. (2.5a).] The one-loop diagrams that contribute to the vertex function are shown in Fig. 1(b); for $m(t)=0$ the second one vanishes and the first one is trivially related to the diagram in the equation of motion. Hence, the renormalized, one-loop expression of (B1) becomes

$$i \int_{t_0}^t dt' \Gamma_q^{(1,1)}(t, t') G_q(t', t_0) = \lambda [q^2 + \tau(t)] G_q(t, t_0) - \frac{1}{4} \lambda \bar{u}_R \{x(t) [q_1(t) + \gamma] + q_2(t)\} G_q(t, t_0), \quad (\text{B2})$$

where $q_1(t)$ and $q_2(t)$ were defined by Eqs. (2.10b) and (2.10c), respectively [with $T(t)$ replacing $X(t)$], and γ is Euler's constant. As in the derivation of the equation of motion for the average order parameter, $q_2(t)$ has not been ϵ expanded (see Appendix A).

The equation for the response function is written in crossover form by performing the same steps as in the equation of motion for the order parameter. Use of the match condition, Eq. (3.6), yields

$$\partial_t G_q(t, t_0) = -[\lambda q^2 + \Lambda(t)T(t) - \frac{1}{4}U(t)Q_2(t)] G_q(t, t_0) + \delta(t - t_0), \quad (\text{B3})$$

where $Q_2(t)$ is defined by Eq. (3.4c), where as before $T(t)$ replaces $X(t)$.

*Author to whom correspondence should be addressed.

¹See, e.g., J. D. Gunton, M. San Miguel, and P. S. Sahni, in *Dynamics of First Order Phase Transitions*, edited by C. Domb and J. L. Lebowitz (Academic, New York, 1984), Vol. VIII; K. Binder, Rep. Prog. Phys. **50**, 783 (1987); H. Furukawa, Adv. Phys. **34**, 703 (1985).

²C. Roland and M. Grant, Phys. Rev. Lett. **60**, 2657 (1988); J. Vinals, M. Grant, M. San Miguel, J. D. Gunton, and E. T. Gawlinski, *ibid.* **54**, 1264 (1985); S. Kumar, J. Vinals, and J. D. Gunton, Phys. Rev. B **34**, 1908 (1986).

³K. R. Elder, T. M. Rogers, and R. C. Desai, Phys. Rev. B **38**, 4725 (1988); T. M. Rogers, K. R. Elder, and R. C. Desai, *ibid.* **37**, 9638 (1988); Y. Oono and S. Puri, Phys. Rev. Lett. **58**, 836 (1987); Y. Oono and S. Puri, Phys. Rev. A **38**, 434 (1988).

⁴G. F. Mazenko, O. T. Valls, and F. C. Zhang, Phys. Rev. B **32**, 5807 (1985); G. F. Mazenko and O. T. Valls, Phys. Rev. Lett. **59**, 680 (1987).

⁵K. Binder, Phys. Rev. B **8**, 3423 (1973).

⁶R. Becker and W. Döring, Ann. Phys. **24**, 719 (1935).

⁷J. W. Cahn, Trans. Metall. Soc. AIME **242**, 166 (1968), and references therein; H. E. Cook, Acta Metall. **18**, 297 (1970); J. S. Langer, Ann. Phys. **65**, 53 (1971).

⁸K. Binder, C. Billotet, and P. Miold, Z. Phys. B **30**, 183 (1978).

⁹K. Kaski, K. Binder, and J. D. Gunton, J. Phys. A **16**, L623 (1983).

¹⁰D. W. Heermann, W. Klein, and D. Stauffer, Phys. Rev. Lett. **49**, 1262 (1982); M. A. Novotny, W. Klein, and P. A. Rikvold, Phys. Rev. B **33**, 7729 (1985).

¹¹H. Horner and K. Jüngling, Z. Phys. B **36**, 97 (1979).

¹²J. S. Langer, M. Bar-on, and H. D. Miller, Phys. Rev. A **11**, 1417 (1975).

¹³C. Billotet and K. Binder, Z. Phys. B **32**, 195 (1979).

¹⁴K. Kawasaki, M. C. Yalabik, and J. D. Gunton, Phys. Rev. A **17**, 455 (1978).

¹⁵G. F. Mazenko, O. T. Valls, and M. Zannetti, Phys. Rev. B **38**, 520 (1988).

¹⁶Y. Drossinos and D. Ronis, Phys. Rev. B **39**, 12078 (1989).

¹⁷O. Penrose and J. L. Lebowitz, J. Stat. Phys. **3**, 211 (1971).

¹⁸J. Rudnick and D. R. Nelson, Phys. Rev. B **13**, 2208 (1976).

¹⁹Moreover, it was shown that considering finite- k , droplet fluctuations did not qualitatively alter our conclusions.

²⁰P. C. Hohenberg and B. I. Halperin, Rev. Mod. Phys. **49**, 435 (1977).

²¹P. C. Martin, E. D. Siggia, and H. A. Rose, Phys. Rev. A **8**, 423 (1973).

²²(a) R. Bausch, H. K. Janssen, and H. Wagner, Z. Phys. B **24**, 113 (1976); (b) R. Bausch and H. K. Janssen, *ibid.* **25**, 275 (1976); (c) R. Bausch, E. Eisenriegler, and H. K. Janssen, *ibid.* **36**, 179 (1979).

²³E. Brézin, J. C. Le Guillou, and J. Zinn-Justin, in *Phase Transitions and Critical Phenomena*, edited by C. Domb and M. S. Green (Academic, New York, 1976), Vol. VI; D. J. Amit, *Field Theory, the Renormalization Group, and Critical Phenomena* (World Scientific, Singapore, 1984).

²⁴G. 't Hooft and M. Veltman, Nucl. Phys. **B44**, 89 (1972); G. 't Hooft, *ibid.* **B62**, 444 (1973); I. D. Lawrie, J. Phys. A **9**, 961 (1976).

²⁵R. V. Jensen, J. Stat. Phys. **25**, 183 (1981).

²⁶Selective ϵ expansion of terms that do not give rise to ϵ^{-1} poles is not new; it has been used in the treatment of Goldstone-mode singularities in the equation of state of the N -vector model; cf. L. Schäfer and H. Horner, Z. Phys. B **29**, 251 (1978).

²⁷Our numerical results suggest that in most cases the difference of the two rescalings is numerically negligible.

²⁸E. Brézin, D. J. Wallace, and K. G. Wilson, Phys. Rev. Lett. **29**, 591 (1972).

²⁹The parameter α ensures that the static one-loop equation of state obeys Griffiths's analyticity [R. B. Griffiths, Phys. Rev. **158**, 176 (1967)]. Moreover, the static equation of state is universal to that order in the ϵ expansion [$dH/d\alpha = O(\epsilon^3)$]; see also Ref. 16.

³⁰An alternate way in which to characterize this component of the structure factor is to consider $q_{\max}(t)$, the maximum of $q^2 S_q(t)$ as suggested by Binder; numerically, while $q_{\max}(t)$ and $q_F(t)$ differ slightly, their scaling properties are equivalent; cf. Fig. 10.

³¹J. S. Langer, Physica **73**, 61 (1974).